AGU ADVANCING EARTH AND SPACE SCIENCE

Geophysical Research Letters

RESEARCH LETTER
10.1029/2021GL092725

Statistical Investigation of the Frequency Dependence of the Chorus Source Mechanism of Plasmaspheric Hiss

Nigel P. Meredith[1], Jacob Bortnik[2], Richard B. Horne[1], Wen Li[3], and Xiao-Chen Shen[3]

[1]British Antarctic Survey, Natural Environment Research Council, Cambridge, England, [2]Department of Atmospheric and Oceanic Sciences, University of California Los Angeles, Los Angeles, CA, USA, [3]Center for Space Physics, Boston University, Boston, MA, USA

Key Points:

- Chorus is an important source of medium frequency plasmaspheric hiss ($200 < f < 2{,}000$ Hz)
- Chorus is unlikely to be the source of low frequency plasmaspheric hiss ($50 < f < 200$ Hz)
- We identify the strong emissions in the 2,000–4,000 Hz band on the dawnside during active conditions as chorus waves outside the plasmapause

Correspondence to:
N. P. Meredith,
nmer@bas.ac.uk

Citation:
Meredith, N. P., Bortnik, J., Horne, R. B., Li, W., & Shen, X.-C. (2021). Statistical investigation of the frequency dependence of the chorus source mechanism of plasmaspheric hiss. *Geophysical Research Letters*, *48*, e2021GL092725. https://doi.org/10.1029/2021GL092725

Received 27 JAN 2021
Accepted 16 FEB 2021

Abstract We use data from eight satellites to statistically examine the role of chorus as a potential source of plasmaspheric hiss. We find that the strong equatorial ($|\lambda_m| < 6°$) chorus wave power in the frequency range $50 < f < 200$ Hz does not extend to high latitudes in any magnetic local time sector and is unlikely to be the source of the low frequency plasmaspheric hiss in this frequency range. In contrast, strong equatorial chorus wave power in the medium frequency range $200 < f < 2{,}000$ Hz is observed to extend to high latitudes and low altitudes in the pre-noon sector, consistent with ray tracing modeling from a chorus source and supporting the chorus to hiss generation mechanism. At higher frequencies, chorus may contribute to the weak plasmaspheric hiss seen on the dayside in the frequency range $2{,}000 < f < 3{,}000$ Hz band but is not responsible for the weak plasmaspheric hiss on the nightside in the frequency range $3{,}000 < f < 4{,}000$ Hz.

Plain Language Summary Plasma waves in space, known as plasmaspheric hiss, are responsible for the formation of the slot region between the inner and outer radiation belt. The waves occur in the frequency range from 20 Hz to several kHz and are typically observed close to the planet in the high density plasmasphere from 2 to 4 R_E(Earth radii) in the magnetic equatorial plane. In this study, we use data from eight satellites to statistically examine the role of a different plasma wave, known as chorus, as a potential source of plasmaspheric hiss. Chorus is observed further from the planet, in a lower density region known as the plasma trough and ranging from 5 to 10 R_E from the planet in the equatorial plane. We find that chorus waves in the frequency range $50 < f < 200$ Hz are well separated from the plasmaspheric hiss closer to the planet and are unlikely to be the source of low frequency plasmaspheric hiss. In contrast, chorus waves in the medium frequency range $200 < f < 2{,}000$ Hz are observed to extend to high latitudes and low altitudes in the pre-noon sector, consistent with ray tracing modeling from a chorus source and supporting the chorus to hiss generation mechanism.

1. Introduction

Plasmaspheric hiss is a broadband, electromagnetic emission that occurs below the electron gyrofrequency in the frequency range from ~20 Hz to several kHz (Li, Ma, et al., 2015). The waves, as their name implies, tend to be confined to the higher density regions associated with the Earth's plasmasphere (e.g., Thorne et al., 1973) and plasmaspheric plumes (e.g., Shi et al., 2019; Summers et al., 2008), where they tend to be strongest on the dayside during geomagnetically active conditions (Li, Ma, et al., 2015; Meredith et al., 2004, 2018).

Plasmaspheric hiss is an important magnetospheric emission due to its role in radiation belt dynamics. It is largely responsible for the formation of the slot region between the inner and outer radiation belt (Lyons & Thorne, 1973). Further out, it contributes to electron loss during geomagnetic storms (Lam et al., 2007) and the quiet time decay of outer radiation belt electrons (Meredith, Horne, Glauert, et al., 2006). It can also explain the slow decay of the unusual narrow ring of multi-MeV electrons produced during the September 2012 geomagnetic storm (Thorne et al., 2013)

Despite over 45 years of research, the origin of plasmaspheric hiss remains a topic of active debate. Ray tracing models show that chorus waves can propagate into the plasmasphere and evolve into plasmaspheric hiss (Bortnik et al., 2008, 2011a, 2011b; Chen et al., 2012a, 2012b; Chen, Li, et al., 2012c). This mechanism is also

supported by observations which confirm some of the key predictions of this theory (Agapitov et al., 2018; Bortnik et al., 2009; Li, Chen, et al., 2015; Meredith et al., 2013; Tsurutani et al., 2012; Wang et al., 2011). However, a recent study has suggested that it is unlikely that chorus directly contributes to a significant fraction of hiss wave power (Hartley et al., 2019). Indeed, there is evidence to suggest that plasmaspheric hiss at low and medium frequencies ($20 < f < 2{,}000$ Hz) can be generated by local amplification of the background whistler mode noise due to substorm injected electrons (Chen et al., 2014; Li et al., 2013; Liu et al., 2020; Su et al., 2018) and, at high frequencies ($f > 2{,}000$ Hz), lightning-generated whistlers also play a role (Meredith, Horne, Clilverd, et al., 2006). Furthermore, He et al. (2019, 2020) have recently reported a new form of high frequency plasmaspheric hiss which they observe to peak on the dawn-side during active conditions and which they also attribute to local generation by substorm injected electrons.

To improve our understanding of the origin of plasmaspheric hiss and, in particular, to examine the role of chorus as a potential source, we extended the ELF/VLF wave database that we originally used to investigate evidence for chorus as the source of plasmaspheric hiss (Meredith et al., 2013) by including ~3 years of data from the Van Allen Probes, Radiation Belt Storm Probes (RBSP)-A and RBSP-B and an additional ~6 years of data from each of the Time History of Events and Macroscale Interactions during Substorms (THEMIS)-A, THEMIS-D and THEMIS-E. The satellites, associated instrumentation, and data analysis techniques used to develop the model are briefly described in Section 2. The global morphology of the average intensities of plasmaspheric hiss as a function of spatial location and frequency are presented and interpreted in Section 3. Finally, our results are discussed and our conclusions presented in Sections 4 and 5, respectively.

2. Instrumentation and Data Analysis

To construct a comprehensive database of plasmaspheric hiss and potentially associated chorus in the inner magnetosphere, we combined data from eight satellites. We used 2.8 years of data from Dynamics Explorer 1, 1 year of data from Double Star TC1, 10 years of data from Cluster 1, 7.8 years of data from THEMIS-A, THEMIS-D, and THEMIS-E, and 2.8 years of data from RBSP-A and RBSP-B. Details of the methods used to analyze the wave data from DE1, Double Star TC1, Cluster 1, and the THEMIS probes are given in Meredith et al. (2012) and those used to analyze the wave data from the Van Allen Probes are given in Li, Ma, et al. (2015).

Magnetosonic waves can potentially contaminate the emissions when the frequency becomes less than the lower hybrid resonance frequency. For the Van Allen Probe measurements, we excluded magnetosonic waves, which typically have large wave normal angles and hence low ellipticity values, by excluding waves with ellipticity less than 0.7. We do not routinely have information on the wave ellipticity from the other satellites and a different approach is required. Observations show that magnetosonic waves are tightly confined to the equatorial region (e.g., Němec et al., 2006), and we remove these waves to first order by excluding emissions below the lower hybrid resonance frequency within ±3° of the geomagnetic equator.

We binned the wave power from each satellite in eight frequency bands between 10 and 4,000 Hz as a function of L^*, magnetic local time (MLT), magnetic latitude (λ_m), and geomagnetic activity as monitored by the *AE* index as detailed in Table 2 in Meredith et al. (2012). For the database, L^* and MLT were computed using the Olson-Pfitzer quiet time model (Olson & Pfitzer, 1977) and the IGRF field at the middle of the appropriate year. Since the software is designed for particles and we are using it for waves we assume a local pitch angle of 90° in the calculation of L^*. We then combined the data from each of the satellites, weighting the data from each individual satellite by the corresponding number of samples, to produce a combined wave database as a function of frequency band, L^*, MLT, λ_m, and geomagnetic activity.

Addition of the new wave data allows us to extend the frequency coverage below 100 Hz enabling us to probe the origins of low frequency plasmaspheric hiss. Furthermore, at higher frequencies, both the statistics and coverage are significantly improved in the near-equatorial region. For example, the average number of samples of the plasma waves in the frequency range $200 < f < 500$ Hz per L^*, MLT bin in the region $|\lambda_m| < 15°$ for $2 < L^* < 8$ during active conditions, $AE > 100$ nT, with and without the new wave data is 23,776 and 661, respectively, increasing the average number of samples in each L^*, MLT bin by a factor of greater than 35. The extended database enables us to examine the global distribution of the wave power in

the near-equatorial region at a latitudinal resolution of 6°, compared with 10° in Li et al. (2011) and 15° in Meredith et al. (2012; 2013), revealing new features.

3. Global Morphology

Chorus waves are typically generated close to the geomagnetic equatorial plane (LeDocq et al., 1998; Santolik & Gurnett 2003) by anisotropic distributions of electrons with energies in the range of approximately keV to ~100 keV (Li et al., 2010; Omura et al., 2008) injected into the inner magnetosphere during storms and substorms. If these chorus emissions are the source of plasmaspheric hiss then we would expect to see clear evidence of chorus extending from its generation region near the geomagnetic equator to higher latitudes and low altitudes where, according to theory, it can enter the plasmasphere and evolve into plasmaspheric hiss (Bortnik et al., 2008). For the purposes of this investigation, we define low, medium, and high frequency plasmaspheric hiss as having frequencies in the ranges $20 < f < 200$, $200 < f < 2{,}000$, and $2{,}000 < f < 4{,}000$ Hz, respectively. We then look for signatures of the chorus to hiss generation mechanism by examining the global distribution of the waves during active conditions, $AE > 100$ nT, as a function of frequency.

To examine the global distribution of the waves, we plot the average wave intensity during active conditions, when the waves tend to be enhanced, as a function of frequency band, λ_m, L^*, and MLT in Figures 1 and 2. To examine the dependence on latitude in more detail, we also plot the global distribution of the waves in the meridional plane as a function of frequency band and MLT sector in Figures 3 and 4. The four frequency bands in the range 20–500 Hz are presented in Figures 1 and 3, and the four frequency bands in the range 500–4,000 Hz are presented in Figures 2 and 4. In the figures, the results are displayed for, from bottom to top, increasing frequency and, from left to right, either increasing magnetic latitude (Figures 1 and 2) or increasing magnetic local time (Figures 3 and 4). The average intensities are shown in the large panels and the corresponding sampling distributions in the small panels. In the meridional plots, Figures 3 and 4, dipole field lines and lines of constant magnetic latitude are included to help visualize the behavior of the wave intensities as a function of L^* and $|\lambda_m|$. We also include the wave data beyond $|\lambda_m| = 18°$, but note that the coverage is much reduced at the higher latitudes.

Two populations of waves can generally be seen in the equatorial region, $|\lambda_m| < 6°$, (e.g., Figure 1a). An inner population which peaks on the dayside inside $L^* = \sim 5$, consistent with previous observations of plasmaspheric hiss (Li, Ma, et al., 2015; Meredith et al., 2004, 2018) and an outer population that peaks further out on the dawnside consistent with previous observations of whistler mode chorus (Li et al., 2011; Meredith et al., 2001, 2020).

3.1. Low Frequency Plasmaspheric Hiss

Strong equatorial ($|\lambda_m| < 6°$) low frequency plasmaspheric hiss in the 100–200 Hz band is observed on the dayside in the region $2.0 < L^* < 5.0$ (Figure 1d). Here, and elsewhere, we define regions of strong wave power as those with average wave intensities greater than 200 pT^2. These regions are color-coded red in the plots. Further out, strong equatorial chorus is observed primarily in the region $6.5 < L^* < 10$ from 22:00 to 08:00 MLT. Moving to higher latitudes, the hiss intensities weaken and the chorus intensities fall off dramatically such that, in the region $12 < |\lambda_m| < 18°$, there is no significant chorus power on the nightside and much reduced power in the region 06:00 to 08:00 MLT (Figure 1f). Moving to even higher latitudes, there is no evidence for strong chorus wave power inside $L^* = 9$ in any MLT sector (Figures 3e–3h). Although not so strong, the observed wave power follows a similar pattern of behavior in the 50–100 Hz band. Here, in the equatorial region, low frequency plasmaspheric hiss is observed primarily on the dayside and weakens with increasing latitude (Figures 1g–1i). Further out, chorus is strongest in the equatorial region at $L^* > 7$ from 23:00 to 07:00 MLT (Figure 1g) and falls off dramatically with increasing latitude (Figures 1h and 1i). Low frequency plasmaspheric hiss is much weaker in the 20–50 Hz band (Figure 1j). However, we are unable to examine chorus at higher L^* since the coverage is limited to $L^* < \sim 6$ due to the exclusion of the THEMIS data, which suffers from variable background noise contamination in this frequency range. These results suggest that chorus is unlikely to be significant source of low frequency plasmaspheric hiss ($50 < f < 200$ Hz) since strong chorus is not observed to extend to high latitudes in any MLT sector. The

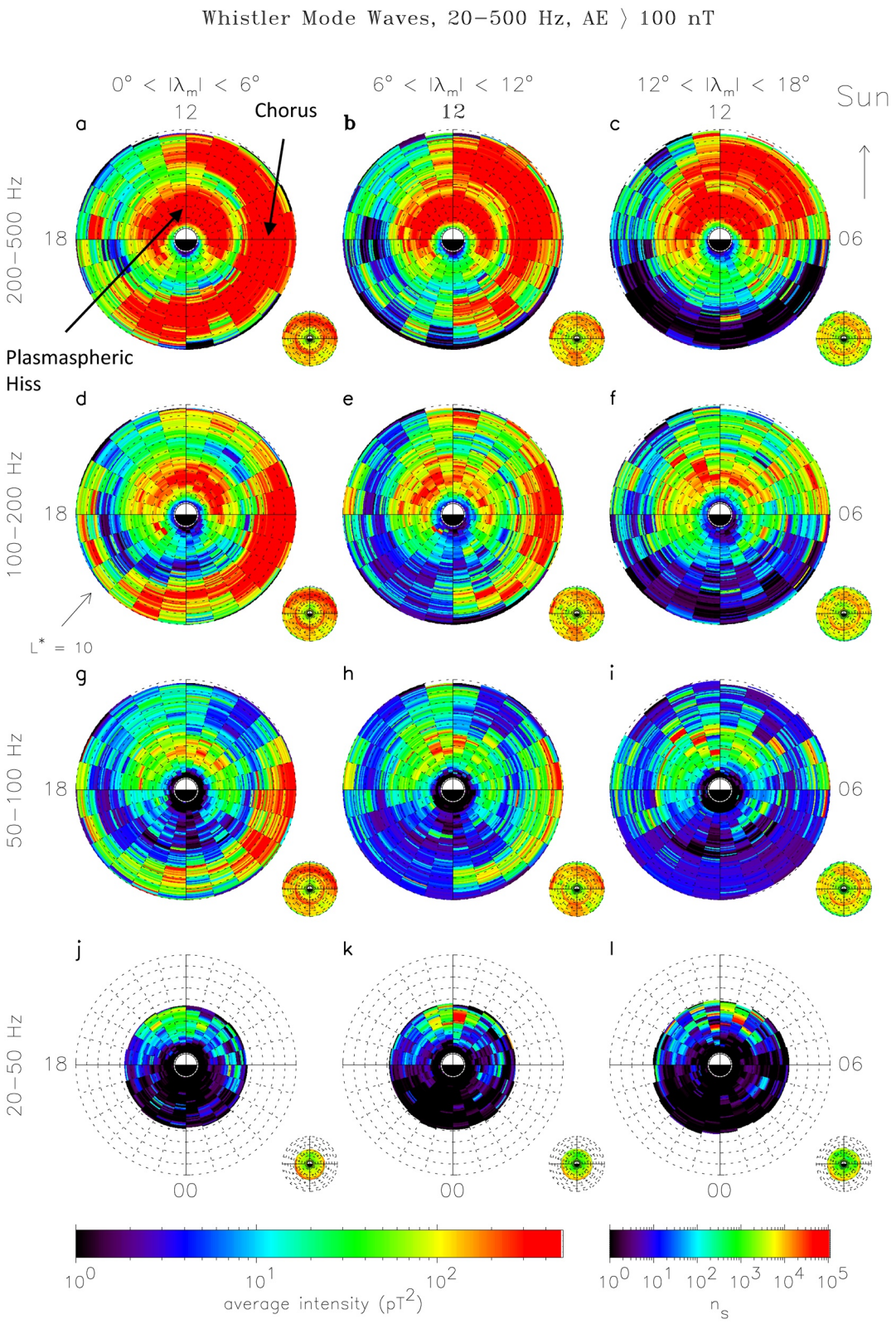

Figure 1. Global maps of the average wave intensity in the frequency range $20 < f < 500$ Hz during active conditions ($AE > 100$ nT) as a function of L^* and MLT for, from bottom to top, increasing frequency band and, from left to right, increasing magnetic latitude. The maps extend linearly out to $L^* = 10$ with noon at the top and dawn to the right. The average intensities are shown in the large panels and the corresponding sampling distributions in the small panels.

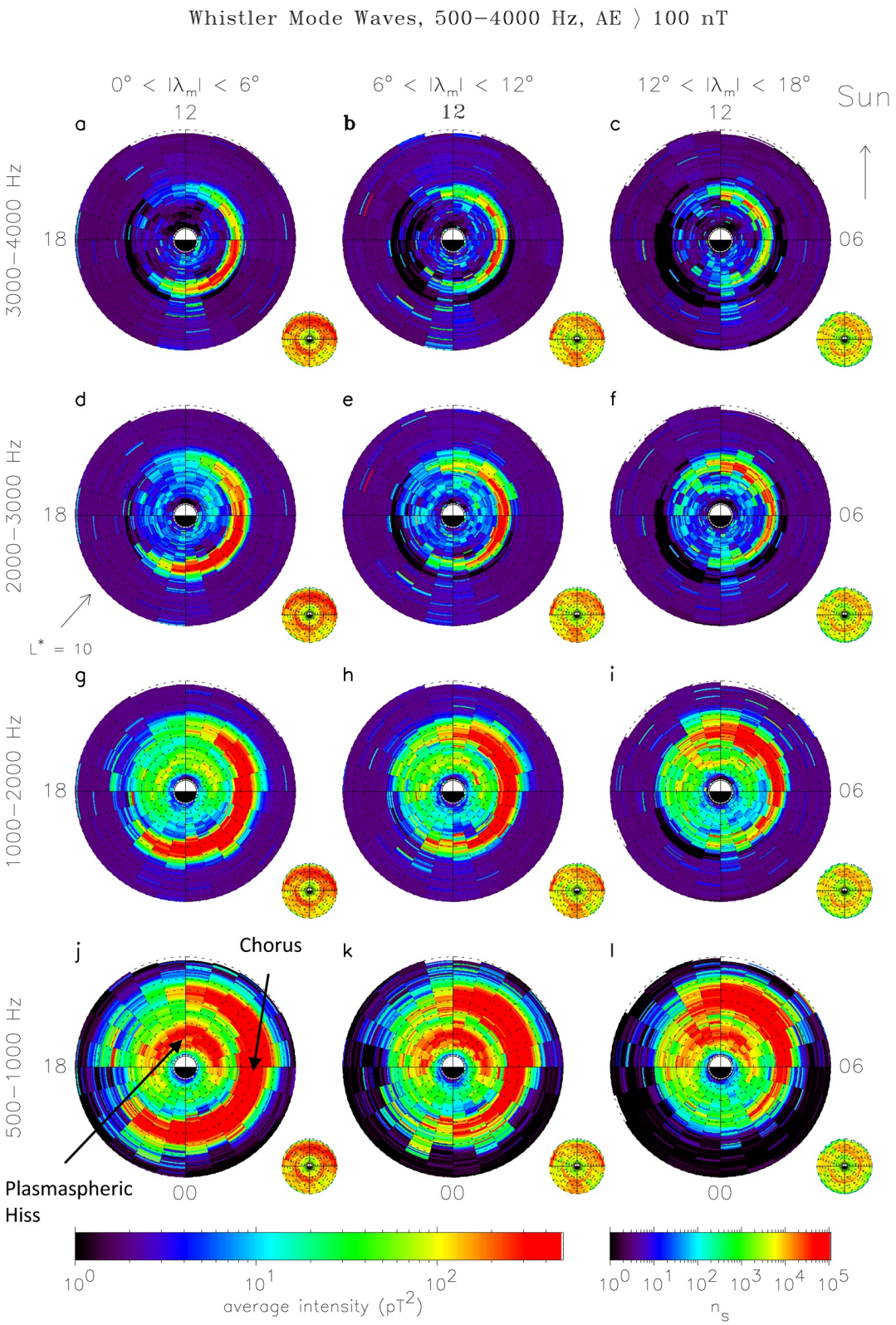

Figure 2. Global maps of the average wave intensity in the frequency range $500 < f < 4{,}000$ Hz during active conditions ($AE > 100$ nT) as a function of L^* and MLT for, from bottom to top, increasing frequency band and, from left to right, increasing magnetic latitude. The maps extend linearly out to $L^* = 10$ with noon at the top and dawn to the right. The average intensities are shown in the large panels and the corresponding sampling distributions in the small panels.

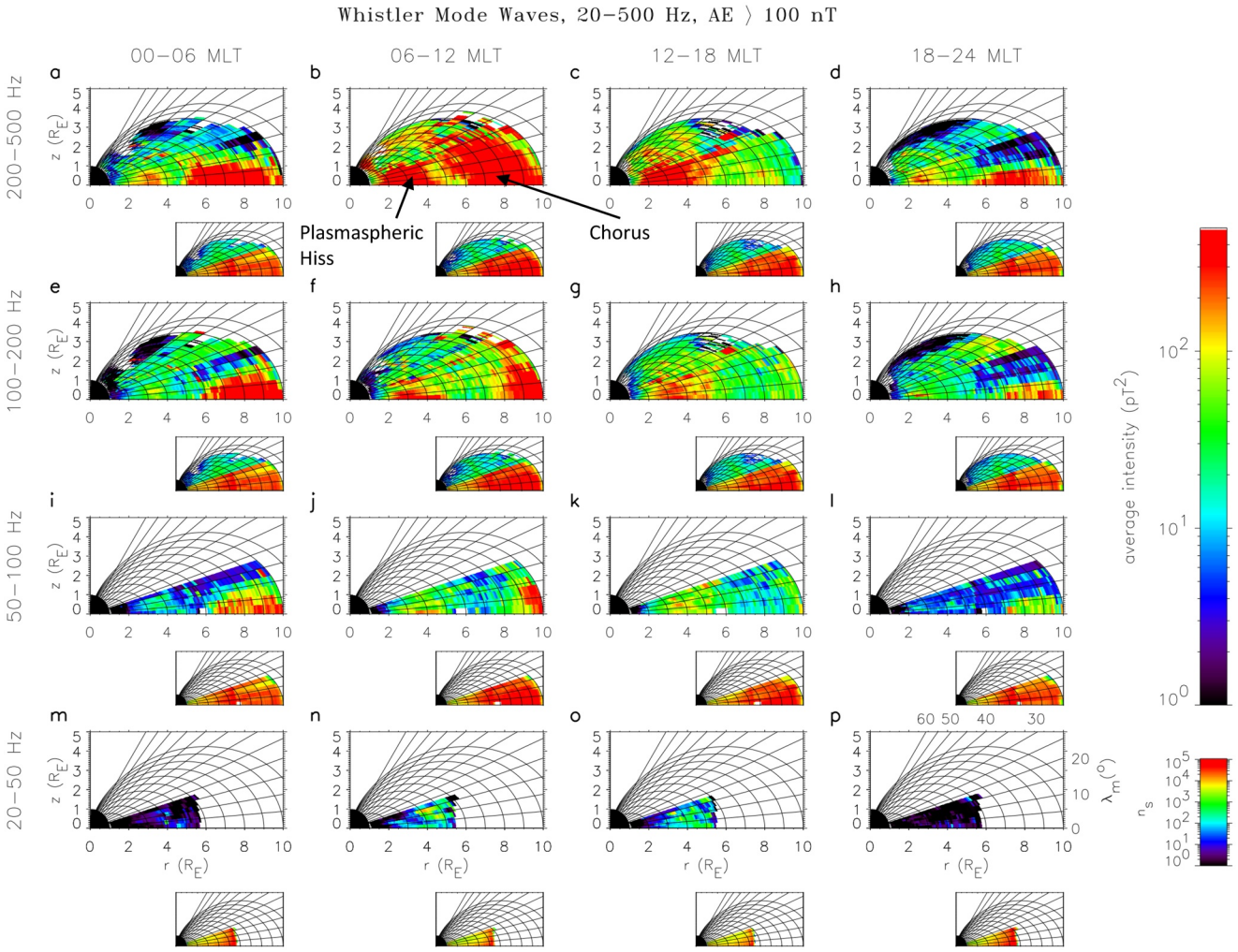

Figure 3. Global maps of the average wave intensity in the frequency range $20 < f < 500$ Hz during active conditions ($AE > 100$ nT) in the meridional plane for, from bottom to top, increasing frequency and, from left to right, increasing MLT. The average intensities are shown in the large panels and the corresponding sampling distributions in the small panels.

source of the low frequency plasmaspheric hiss in this frequency range is more likely to be local amplification of the background whistler mode noise due to substorm-injected electrons in the outer plasmasphere (e.g., Chen et al., 2014; Li et al., 2013).

3.2. Medium Frequency Plasmaspheric Hiss

Strong equatorial medium frequency plasmaspheric hiss in the 200–500 Hz band is observed in the equatorial region on the dayside from $1.5 < L^* < 5.0$ (Figure 1a). The region of strong waves also extends for a few hours into the pre-dawn and post dusk sectors, albeit for smaller ranges of L^*. Further out, strong equatorial chorus is observed from 21:00 MLT through dawn to 13:00 MLT primarily in the region $5 < L^* < 10$, with the inner boundary of the strong chorus moving progressively to larger values of L^* with decreasing and increasing MLT in the pre-midnight and pre-noon sectors, respectively (Figure 1a). Moving to higher latitudes the plasmaspheric hiss remains strong (Figures 1b and 1c). The chorus intensities also remain strong in the pre-noon sector where they are also observed to extend to lower L^* (Figures 1b and 1c). In fact, strong waves are observed all the way from the equator to very high latitudes in the region $5 < L^* < 7$ in the pre-noon sector (Figure 3b). Indeed, a second intensity peak is seen at high latitudes and low altitudes due to the convergence of the magnetic field lines. On the nightside, the strong chorus is tightly confined to the equatorial

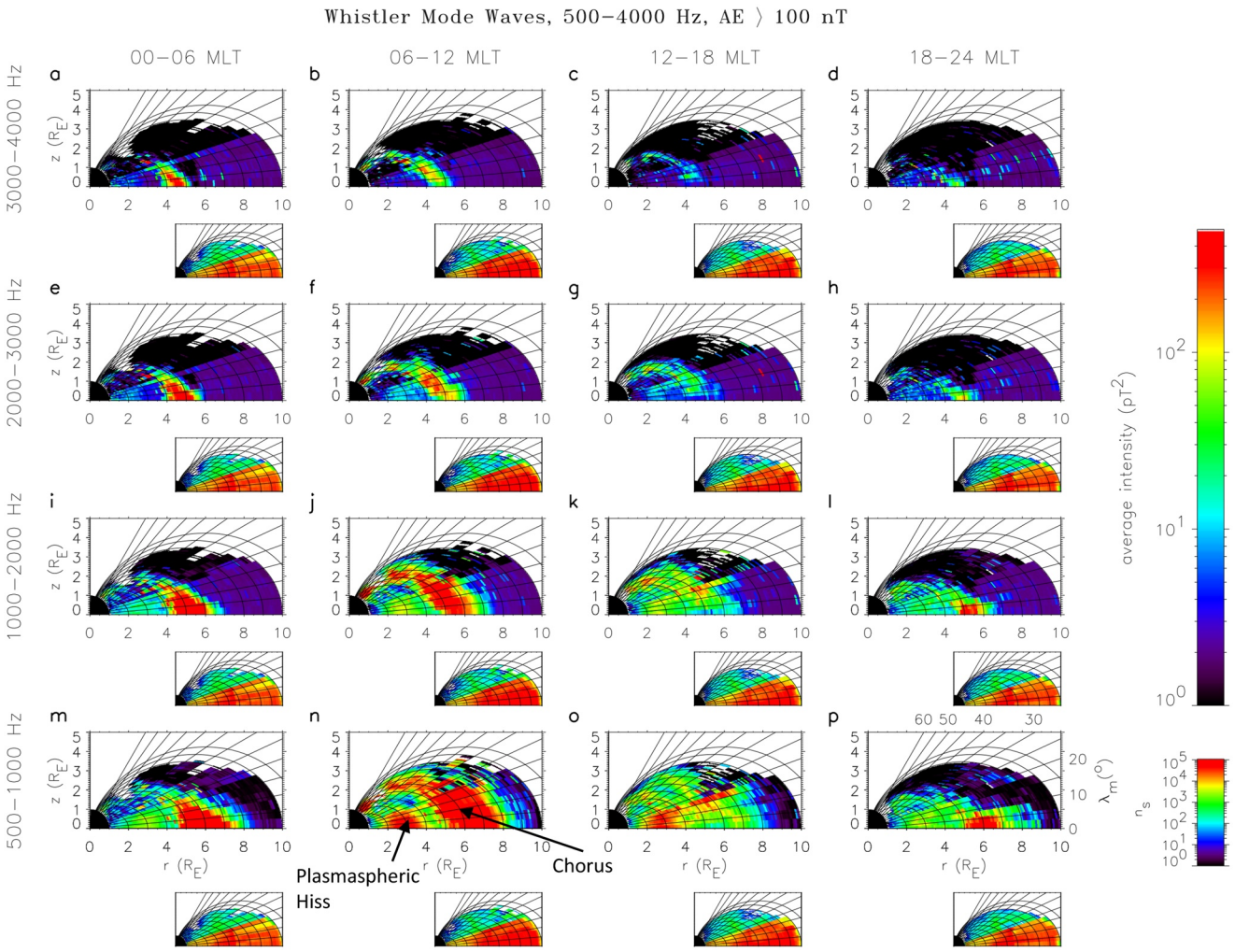

Figure 4. Global maps of the average wave intensity in the frequency range $500 < f < 4{,}000$ Hz during active conditions ($AE > 100$ nT) in the meridional plane for, from bottom to top, increasing frequency and, from left to right, increasing MLT. The average intensities are shown in the large panels and the corresponding sampling distributions in the small panels.

region, being largely restricted to the regions $|\lambda_m| < 6°$ and $|\lambda_m| < 12°$ in the pre- and post-midnight sectors, respectively (Figures 3d and 3a).

We observe a similar pattern of behavior for medium frequency plasmaspheric hiss in the 500–1,000 Hz band, although the overall extent of the regions of strong plasmaspheric hiss and chorus are reduced (Figure 2j). For example, in this frequency range the strong equatorial plasmaspheric hiss is observed primarily on the dayside in the region $2 < L^* < 4$. Strong equatorial chorus is observed from 21:00 MLT through dawn to noon but the spatial extent is restricted to the range $5 < L^* < 8$. Unlike the situation at lower frequencies strong waves are absent in the region $8 < L^* < 10$. Moving to higher latitudes plasmaspheric hiss remains strong on the dayside (Figures 2k and 2l). The chorus intensities remain strong in the pre-noon sector (Figures 2k and 2l) and intensify post-noon from 12:00 to 14:00 MLT in the range $5 < L^* < 7$ (Figure 2l). The chorus also remains strong in a restricted zone in the pre-dawn sector from 02:00 to 06:00 MLT in the region $5 < L^* < 6$ for $12 < \lambda_m < 18°$. Moving further from the equator, strong waves are observed to extend to high latitudes and low altitudes in the region $5 < L^* < 7$ in the pre-noon sector (Figure 4n).

Medium frequency plasmaspheric hiss is weaker in the 1,000–2,000 Hz band, with intensities of the order of 100 pT^2 on the dayside (Figure 2g). Strong equatorial chorus is still observed further out, although it is more tightly confined, being observed from 21:00 MLT through dawn to 10:00 MLT, typically from $4.5 < L^* < 6$. Moving away from the equator, the strong chorus is mostly confined to the region 03:00 to 14:00 MLT for

$12 < \lambda_m < 18°$ (Figure 2i). Chorus remains strong in the region $4.5 < L^* < 6$ to high latitudes and low altitudes, but only in the pre-noon sector (Figure 4j).

Our statistical observations demonstrate that strong chorus waves in the frequency range $200 < f < 2{,}000$ Hz are present all the way from the equatorial region to high latitudes and low altitudes in the pre-noon sector, consistent with ray tracing studies from an equatorial chorus source region (Bortnik et al., 2007). The intensity of plasmaspheric hiss is weaker in the 1,000–2,000 Hz band despite strong chorus being present further out, and this is consistent with ray tracing theory which suggests that waves have more difficulty accessing the plasmasphere at higher frequencies (Bortnik et al., 2007). We note that strong hiss is observed in the afternoon sector with no immediate counterpart in chorus activity in the same meridional plane at higher L^*. However, off-meridional propagation can be very effective in the afternoon sector during geomagnetic storms due to strong azimuthal plasma density gradients enabling rays to propagate eastwards where they can potentially explain the strong plasmaspheric hiss emissions in the post-noon sector during active times (Chen et al., 2009).

3.3. High Frequency Plasmaspheric Hiss

High frequency plasmaspheric hiss is much weaker than both low and medium frequency plasmaspheric hiss, and becomes weaker with increasing frequency. In the 2,000–3,000 Hz band intensities of the order 10 pT^2 are observed on the dayside in the region $2.0 < L^* < 4.0$ (Figure 2d). Further out, strong equatorial chorus intensities are observed from 23:00 to 09:00 MLT, typically from $4.0 < L^* < 5.5$. Moving away from the equator, the strong chorus is mostly confined to the region 03:00 to 12:00 MLT for $12 < \lambda_m < 18°$ (Figure 2f). The strong chorus wave power does not extend to higher latitudes although weaker levels of chorus power extend to low altitudes in the region $4 < L^* < 5$ on the dayside (Figures 4f and 4g). At higher frequencies, 3,000–4,000 Hz, the high frequency plasmaspheric hiss wave power is even weaker, with largest intensities less than a few pT^2 on the dayside. Here, the intensities peak on the nightside rather than the dayside suggesting a different source. Strong equatorial chorus is observed from 23:00 to 09:00 MLT, typically from $4.0 < L^* < 5.0$ (Figure 2a) with the region of strong wave power moving progressively to larger MLT with increasing latitude (Figures 2c and 2d). Weak power extends to high latitudes in the pre-noon sector in the region $4 < L^* < 5$, but it is not related to any significant levels of plasmaspheric hiss inside the plasmapause. These results suggest that chorus may contribute to the observed intensities in the 2,000–3,000 Hz band but not at higher frequencies where the distribution of the wave power is completely different. This weaker population of high frequency plasmaspheric hiss on the nightside is more likely to be produced by lightning generated whistlers (e.g., Meredith, Horne, Clilverd, et al., 2006).

4. Discussion

The new study reveals some interesting features in the global distribution of chorus in the pre-dawn sector. Here, the waves tend to extend to higher latitudes at lower L^* for frequencies above 500 Hz. For example, at $L^* = 7$, 6, and 5 the strongest waves in the 500–1,000 Hz band are confined to within 6, 12, and 18°, respectively (Figure 4m). Moving to higher frequencies, for any given L^* the strong equatorial chorus, if present, tends to be more tightly confined to the equatorial plane (Figures 4i, 4e and 4a). However, at lower frequencies the chorus tends to be mostly confined to within 9° of the geomagnetic equator (Figures 3a, 3e and 3i). In contrast, in the pre-noon sector, the waves can extend to much higher latitudes (Figures 3b, 4n, 4j, and 4f). We suggest that the behavior of the chorus wave power outside the generation region is dominated by Landau damping which is less efficient at higher frequencies and higher values of L^* and less efficient in the pre-noon sector (Bortnik et al., 2007).

He et al. (2020) recently conducted a statistical survey of high frequency plasmaspheric hiss, first reported in He et al. (2019), and showed evidence for enhanced waves in the plasmasphere on the dawnside during active conditions. Specifically, they showed evidence for enhanced wave power in the frequency band from 2000 Hz to $0.5f_{ce}$ which increased with increasing geomagnetic activity and also moved to lower L^* with increasing geomagnetic activity. We see no evidence for enhanced plasmaspheric hiss at high frequencies in the dawn sector. We do, however, see evidence of enhanced chorus in this region. While we do not discriminate between the waves inside and outside of the plasmapause in this study, in previous work, we

demonstrated that the plasmapause is typically around $L = 4.5$ in the pre-dawn sector during active conditions (Meredith et al., 2004, 2008). Furthermore, the general inward movement of the region of enhanced chorus emissions with increasing frequency (Figures 1a, 1d and 2a, 2d, 2g, 2j) is consistent with its dependence on the electron gyrofrequency which increases with decreasing L (see, e.g., Figure 3 in Meredith et al., 2013). Our observations suggest that the strong waves at frequencies in the 2,000–4,000 Hz bands in the region $4.0 < L^* < 5.5$ on the dawnside (Figures 2a and 2d) are chorus waves outside the plasmapause. The results also suggest that the waves observed at $f > 2{,}000$ Hz on the dawnside at $L > 4.0$ during active conditions by He et al. (2020) are predominantly chorus waves outside the plasmasphere.

Hartley et al. (2019) recently suggested that chorus waves rarely exist with the wave vector orientation required to enter the plasmasphere and that the waves that are observed with the orientation required to propagate into the plasmasphere do not carry a substantial fraction of the wave power, bringing into question the efficacy of the chorus to hiss mechanism. However, our statistical study reveals strong wave power at high latitudes and low altitudes in the frequency range $200 < f < 2{,}000$ Hz linked to strong equatorial chorus wave power. The results suggest that significant chorus power can propagate to these locations, from where, according to theory, the waves can enter the plasmasphere and evolve into plasmaspheric hiss (Bortnik et al., 2008). The reason for the disparity in these contradictory conclusions could be related to the method used to calculate the wave normal angles in the Hartley et al. (2019) study. The wave normal angles are derived from 486 m s waveforms recorded every 6 s and do not capture the full chorus elements or examine them in detail. To take into account, the variability of the wave vector orientation Hartley et al. (2019) assumed a 20° wide distribution of wave normal angles and azimuthal angles centered on the mean values. However, this technique does not capture the full range of wave vector orientations that can be present in a chorus element. For example, Santolik et al. (2014) conducted a systematic analysis of 2,230 chorus subpackets in the morning-side equatorial region at $R \sim 5$ Earth radii and showed that waves in the frequency range $0.2f_{ce} < f < 0.4f_{ce}$ with large amplitudes, of the order of hundreds of pT, can extend to wave normal angles of 30° and above. More recently, Crabtree et al. (2017), using Bayesian spectral analysis, found that after the first chorus few sub-elements, the wave normal angle and azimuthal angle change continuously within each sub-element, extending to intermediate wave normal angles and covering the full range of azimuthal angles. To comprehensively examine the chorus to hiss mechanism using wave vector orientations in the near-equatorial plane, a thorough analysis of the fine structure of the chorus wave normal and azimuthal angles would be required.

5. Conclusions

We have used our extended database of ELF/VLF waves to statistically examine the role of chorus as the source of plasmaspheric hiss. Our principal conclusions are:

1. Strong equatorial chorus observed during active conditions in the frequency range $50 < f < 200$ Hz is not observed to extend to high latitudes and is thus not likely to be the source of low frequency plasmaspheric hiss
2. Strong equatorial chorus observed during active conditions in the frequency range $200 < f < 2{,}000$ Hz is observed to extend to higher latitudes and low altitudes, principally in the pre-noon sector, consistent with ray tracing modeling from a chorus source, suggesting that chorus is an important source of medium frequency plasmaspheric hiss
3. Chorus in the frequency range $2{,}000 < f < 3{,}000$ Hz is observed to extend to higher latitudes albeit at much weaker levels, principally in the pre-noon sector during active times, where it may contribute to the weak plasmaspheric hiss seen on the dayside.
4. Chorus does not extend to high latitudes on the nightside in any frequency range and is unlikely to be the source of the very weak plasmaspheric hiss observed primarily on the nightside in the frequency range $3{,}000 < f < 4{,}000$ Hz

Data Availability Statement

The results and data shown in this study can be downloaded from the UK Polar Data Center (https://data.bas.ac.uk and https://doi.org/10.5285/151a855f-d030-485b-a2dd-4ea874e59bf6).

Acknowledgments
We acknowledge the CDAWeb (https://cdaweb.sci.gsfc.nasa.gov/index.html/) for the provision of the DE-1 wave data. The authors thank LPCEE laboratory (Orléans, France) for their help in the analysis of this wave data. The authors thank the STAFF-DWP instrument team for provision of the Double Star TC1 data which is available at the Cluster Science Archive (https://www.cosmos.esa.int/web/csa). The authors thank NASA contract NAS5-02099 and V. Angelopoulos for use of data from THEMIS Mission. Specifically, the authors thank O. Le Contel and A. Roux for use of SCM data, which is available from http://themis.ssl.berkeley.edu/data/themis/. The authors are grateful for the Van Allen Probes data from the EMFISIS instrument obtained from https://emfisis.physics.uiowa.edu/data/index. The authors acknowledge the NSSDC Omniweb for the provision of the geomagnetic activity indices used in this report. The research leading to these results has received funding from the Natural Environment Research Council Highlight Topic grant NE/P01738X/1 (Rad-Sat) and the NERC grants NE/V00249X/1 (Sat-Risk) and NE/R016038/1. J. Bortnik would like to acknowledge support from NASA grant NNX14AI18G, and RBSP-ECT and EMFISIS funding provided by JHU/APL contracts 967399 and 921647 under NASA's prime contract NAS5-01072. W. Li and X.-C. Shen would like to acknowledge support from NASA grants 80NSSC20K0698 and 80NSSC19K0845, NSF grant AGS-1847818, and the Alfred P. Sloan Research Fellowship FG-2018-10936.

References

Agapitov, O., Mourenas, D., Artemyev, A., Mozer, F. S., Bonnell, J. W., Angelopoulos, V., et al. (2018). Spatial extent and temporal correlation of chorus and hiss: Statistical results from multipoint THEMIS observations. *Journal of Geophysical Research: Space Physics*, *123*, 8317–8330. https://doi.org/10.1029/2018JA025725

Bortnik, J., Chen, L., Li, W., Thorne, R. M., & Horne, R. B. (2011). Modeling the evolution of chorus waves into plasmaspheric hiss. *Journal of Geophysical Research*, *116*. A08221. https://doi.org/10.1029/2011JA016499

Bortnik, J., Chen, L., Li, W., Thorne, R. M., Meredith, N. P., & Horne, R. B. (2011). Modeling the wave power distribution and characteristics of plasmaspheric hiss. *Journal of Geophysical Research*, *116*. A12209. https://doi.org/10.1029/2011JA016862

Bortnik, J., Li, W., Thorne, R. M., Angelopoulos, V., Cully, C., Bonnell, J., et al. (2009). An observation linking the origin of plasmaspheric hiss to discrete chorus emissions. *Science*, *324*(5928), 775–778. https://doi.org/10.1126/science.1171273

Bortnik, J., Thorne, R. M., & Meredith, N. P. (2007). Modeling the propagation characteristics of chorus using CRRES suprathermal electron fluxes. *Journal of Geophysical Research*, *112*. A08204. https://doi.org/10.1029/2006JA012237

Bortnik, J., Thorne, R. M., & Meredith, N. P. (2008). The unexpected origin of plasmaspheric hiss from discrete chorus emissions. *Nature*, *452*, 62–66. https://doi.org/10.1038/nature06741

Chen, L., Bortnik, J., Li, W., Thorne, R. M., & Horne, R. B. (2012). Modeling the properties of plasmaspheric hiss: 1. Dependence on chorus wave emission. *Journal of Geophysical Research*, *117*. A05201. https://doi.org/10.1029/2011JA017201

Chen, L., Bortnik, J., Li, W., Thorne, R. M., & Horne, R. B. (2012). Modeling the properties of plasmaspheric hiss: 2. Dependence on the plasma density distribution. *Journal of Geophysical Research*, *117*. A05202. https://doi.org/10.1029/2011JA017202

Chen, L., Bortnik, J., Thorne, R. M., Horne, R. B., & Jordanova, V. K. (2009), Three-dimensional ray tracing of VLF waves in a magnetospheric environment containing a plasmaspheric plume, *Geophysical Research Letters*, *36*, L22101. https://doi.org/10.1029/2009GL040451

Chen, L., Li, W., Bortnik, J., & Thorne, R. M. (2012). Amplification of whistler-mode hiss inside the plasmasphere. *Geophysical Research Letters*, *39*. L08111. https://doi.org/10.1029/2012GL051488

Chen, L., Thorne, R. M., Bortnik, J., Li, W., Horne, R. B., Reeves, G. D., et al. (2014). Generation of unusually low frequency plasmaspheric hiss. *Geophysical Research Letters*, *41*, 5702–5709. https://doi.org/10.1002/2014GL060628

Crabtree, C., Tejero, E., Ganguli, G., Hospodarsky, G. B., & Kletzing, C. A. (2017). Bayesian spectral analysis of chorus subelements from the Van Allen Probes. *Journal of Geophysical Research: Space Physics*, *122*, 6088–6106. https://doi.org/10.1002/2016JA023547

Hartley, D. P., Kletzing, C. A., Chen, L., Horne, R. B., & Santol, O. (2019). Van Allen Probes observations of chorus wave vector orientations: Implications for the chorus-to-hiss mechanism. *Geophysical Research Letters*, *46*, 2337–2346. https://doi.org/10.1029/2019GL082111

He, Z., Chen, L., Liu, X., Zhu, H., Liu, S., Gao, Z., & Cao, Y. (2019). Local generation of high-frequency plasmaspheric hiss observed by Van Allen Probes. *Geophysical Research Letters*, *46*, 1141–1148. https://doi.org/10.1029/2018GL081578

He, Z., Yu, J., Chen, L., Xia, Z., Wang, W., Li, K., & Cui, J. (2020). Statistical study on locally generated high-frequency plasmaspheric hiss and its effect on suprathermal electrons: Van Allen Probes observation and quasi-linear simulation. *Journal of Geophysical Research: Space Physics*, *125*. e2020JA028526. https://doi.org/10.1029/2020JA028526

Lam, M. M., Horne, R. B., Meredith, N. P., & Glauert, S. A. (2007). Modeling the effects of radial diffusion and plasmaspheric hiss on outer radiation belt electrons. *Geophysical Research Letters*, *34*. L20112. https://doi.org/10.1029/2007GL031598

LeDocq, M. J., Gurnett, D. A., & Hospodarsky, G. B. (1998). Chorus source locations from VLF Poynting flux measurements with the Polar spacecraft. *Geophysical Research Letters*, *25*, 4063–4066. https://doi.org/10.1029/1998GL900071

Li, W., Bortnik, J., Thorne, R. M., & Angelopoulos, V. (2011). Global distribution of wave amplitudes and wave normal angles of chorus waves using THEMIS wave observations. *Journal of Geophysical Research*, *116*. A12205. https://doi.org/10.1029/2011JA017035

Li, W., Chen, L., Bortnik, J., Thorne, R. M., Angelopoulos, V., Kletzing, C. A., et al. (2015). First evidence for chorus at a large geocentric distance as a source of plasmaspheric hiss: Coordinated THEMIS and Van Allen Probes observation. *Geophysical Research Letters*, *42*, 241–248. https://doi.org/10.1002/2014GL062832

Li, W., Ma, Q., Thorne, R. M., Bortnik, J., Kletzing, C. A., Kurth, W. S., et al. (2015). Statistical properties of plasmaspheric hiss derived from Van Allen Probes data and their effects on radiation belt electron dynamics. *Journal of Geophysical Research: Space Physics*, *120*, 3393–3405. https://doi.org/10.1002/2015JA021048

Li, W., Throne, R. M., Bortnik, J., Reeves, G. D., Kletzing, C. A., Kurth, W. S., et al. (2013). An unusual enhancement of low-frequency plasmaspheric hiss in the outer plasmasphere associated with substorm-injected electrons. *Geophysical Research Letters*, *40*, 3798–3803. https://doi.org/10.1002/grl.50787

Li, W., Thorne, R. M., Nishimura, Y., Bortnik, J., Angelopoulos, V., McFadden, J. P., et al. (2010). THEMIS analysis of observed equatorial electron distributions responsible for the chorus excitation. *Journal of Geophysical Research*, *115*. A00F11. https://doi.org/10.1029/2009JA014845

Liu, N., Su, Z., Gao, Z., Zheng, H., Wang, Y., Wang, S., et al. (2020). Comprehensive observations of substorm-enhanced plasmaspheric hiss generation, propagation, and dissipation. *Geophysical Research Letters*, *47*. e2019GL086040. https://doi.org/10.1029/2019GL086040

Lyons, L. R., & Thorne, R. M. (1973). Equilibrium structure of radiation belt electrons. *Journal of Geophysical Research*, *78*(13), 2142–2149. https://doi.org/10.1029/JA078i013p02142

Meredith, N. P., Horne, R. B., & Anderson, R. R. (2001). Substorm dependence of chorus amplitudes: Implications for the acceleration of electrons to relativistic energies. *Journal of Geophysical Research*, *106*(A7), 13165–13178. https://doi.org/10.1029/2000JA900156

Meredith, N. P., Horne, R. B., & Anderson, R. R. (2008). Survey of magnetosonic waves and proton ring distributions in the Earth's inner magnetosphere, *Journal of Geophysical Research*, *113*, A06213. https://doi.org/10.1029/2007JA012975

Meredith, N. P., Horne, R. B., Bortnik, J., Thorne, R. M., Chen, L., Li, W., & Sicard-Piet, A. (2013). Global statistical evidence for chorus as the embryonic source of plasmaspheric hiss. *Geophysical Research Letters*, *40*, 2891–2896. https://doi.org/10.1002/grl.50593

Meredith, N. P., Horne, R. B., Clilverd, M. A., Horsfall, D., Thorne, R. M., & Anderson, R. R. (2006). Origins of plasmaspheric hiss. *Journal of Geophysical Research*, *111*. A09217. https://doi.org/10.1029/2006JA011707

Meredith, N. P., Horne, R. B., Glauert, S. A., Thorne, R. M., Summers, D., Albert, J. M., & Anderson, R. R. (2006). Energetic outer zone electron loss timescales during low geomagnetic activity. *Journal of Geophysical Research*, *111*. A05212. https://doi.org/10.1029/2005JA011516

Meredith, N. P., Horne, R. B., Kersten, T., Li, W., Bortnik, J., Sicard, A., & Yearby, K. H. (2018). Global model of plasmaspheric hiss from multiple satellite observations. *Journal of Geophysical Research: Space Physics*, *123*, 4526–4541. https://doi.org/10.1029/2018JA025226

Meredith, N. P., Horne, R. B., Shen, X.-C., Li, W., & Bortnik, J. (2020). Global model of whistler mode chorus in the near-equatorial region ($|\lambda_m| < 18°$). *Geophysical Research Letters*, *47*. https://doi.org/10.1029/2020GL087311

Meredith, N. P., Horne, R. B., Sicard-Piet, A., Boscher, D., Yearby, K. H., Li, W., & Thorne, R. M. (2012). Global model of lower band and upper band chorus from multiple satellite observations. *Journal of Geophysical Research*, *117*. A10225. https://doi.org/10.1029/2012JA017978

Meredith, N. P., Horne, R. B., Thorne, R. M., Summers, D., & Anderson, R. R. (2004). Substorm dependence of plasmaspheric hiss. *Journal of Geophysical Research*, *109*. A06209. https://doi.org/10.1029/2004JA010387

Němec, F., Santolík, O., Gereová, K., Macúsová, E., Laakso, H., de Conchy, Y., et al. (2006). Equatorial noise: Statistical study of its localization and the derived number density. *Advances in Space Research*, *37*, 610–616. https://doi.org/10.1016/j.asr.2005.03.025

Olson, W. P., & Pfitzer, K. (1977). *Magnetospheric magnetic field modeling annual scientific report, AFOSR Contract No. F44620-75-c-0033*.

Omura, Y., Katoh, Y., & Summers, D. (2008). Theory and simulation of the generation of whistler-mode chorus. *Journal of Geophysical Research*, *113*. A04223. https://doi.org/10.1029/2007JA012622

Santolík, O., Gurnett, D. A., Pickett, J. S., Parrot, M., & Cornilleau-Wehrlin, N. (2003). Spatio-temporal structure of storm-time chorus. *Journal of Geophysical Research*, *108*, 1278. https://doi.org/10.1029/2002JA009791

Santolík, O., Kletzing, C. A., Kurth, W. S., Hospodarsky, G. B., & Bounds, S. R. (2014). Fine structure of large-amplitude chorus wave packets. *Geophysical Research Letters*, *41*, 293–299. https://doi.org/10.1002/2013GL058889

Shi, R., Li, W., Ma, Q., Green, A., Kletzing, C. A., Kurth, W. S., et al. (2019). Properties of whistler mode waves in Earth's plasmasphere and plumes. *Journal of Geophysical Research: Space Physics*, *124*, 1035–1051. https://doi.org/10.1029/2018JA026041

Su, Z., Liu, N., Zheng, H., Wang, Y., & Wang, S. (2018). Multipoint observations of nightside plasmaspheric hiss generated by substorm-injected electrons. *Geophysical Research Letters*, *45*, 10921–10932. https://doi.org/10.1029/2018GL079927

Summers, D., Ni, B., Meredith, N. P., Horne, R. B., Thorne, R. M., Moldwin, M. B., & Anderson, R. R. (2008). Electron scattering by whistler-mode ELF hiss in plasmaspheric plumes. *Journal of Geophysical Research*, *113*. A04219. https://doi.org/10.1029/2007JA012678

Thorne, R. M., Li, W., Ni, B., Ma, Q., Bortnik, J., Baker, D. N., et al. (2013). Evolution and slow decay of an unusual narrow ring of relativistic electrons near L∼3.2 following the September 2012 magnetic storm. *Geophysical Research Letters*, *40*, 3507–3511. https://doi.org/10.1002/grl.50627

Thorne, R. M., Smith, E. J., Burton, R. K., & Holzer, R. E. (1973). Plasmaspheric hiss. *Journal of Geophysical Research*, *78*(10), 1581–1596. https://doi.org/10.1029/JA078i010p01581

Tsurutani, B. T., Falkowski, B. J., Verkhoglyadova, O. P., Pickett, J. S., Santol, O., & Lakhina, G. S. (2012). Dayside ELF electromagnetic wave survey: A Polar statistical study of chorus and hiss. *Journal of Geophysical Research*, *117*. A00L12. https://doi.org/10.1029/2011JA017180

Wang, C., Zong, Q., Xiao, F., Su, Z., Wang, Y., & Yue, C. (2011). The relations between magnetospheric chorus and hiss inside and outside the plasmasphere boundary layer: Cluster observation. *Journal of Geophysical Research*, *116*. A07221. https://doi.org/10.1029/2010JA016240